JOURNAL OF MATERIALS SCIENCE 30 (1995) 4986–4993

Fracture toughness of sub-zero-chilled cast iron

K. H. W. SEAH
Department of Mechanical Engineering, National University of Singapore, 10 Kent Ridge Crescent, Singapore 0511

J. HEMANTH, S. C. SHARMA
Department of Mechanical Engineering, R.V. College of Engineering, Mysore Road, Bangalore 560 059, Karnataka, India

A series of fracture toughness experiments were carried out involving sub-zero-chilled (using liquid nitrogen) cast iron containing 1.5% Cu, and chromium contents ranging from 0.0%–0.2%. By using copper chills of different thicknesses, the effect on fracture toughness of varying the chill rate was also examined. The fracture toughness tests were carried out using three-point bend specimens, each with a chevron notch, as per ASTM E 399-1974 standards. It was found that fracture toughness is highly dependent on the location on the casting from where the test specimens are taken and also on the chromium content of the material. Chill thickness, however, does not significantly affect the fracture toughness of the material. There was found to be an approximately linear relationship between fracture toughness and pearlite content, in which fracture toughness increases as pearlite content decreases and vice versa.

1. Introduction

1.1. Chilled cast iron

Chilled cast iron belongs to a group of metals possessing high strength, high hardness and high wear resistance. They are widely used in the manufacture of wear shoes, wear liners, rollers, brake shoes, crushing jaws, grinding mill liners, cam surfaces, wearing plates, and other machine components and equipment requiring such material characteristics. For the design engineer, there are sufficient data available on the mechanical properties of ordinary grey cast iron and alloyed cast iron. However, there is a dearth of information on the fracture properties of sub-zero-chilled cast iron. This has prompted us to embark upon a series of experiments to determine the fracture toughness properties of sub-zero-chilled (using liquid nitrogen) cast iron containing 1.5% Cu, and of chromium contents ranging from 0.0%–0.2%. The reason behind the selection of this series of cast iron for the present investigation is that a wide range of mechanical properties can be obtained with different microstructures. The presence of copper as an alloying element improves the machinability of the cast iron. Moreover, a low-grade cast iron can be converted into one of superior qualities by sub-zero chilling with little or no further addition of alloying elements. In addition, chilling, in the case of cast iron, promotes directional solidification and eliminates shrinkage, porosity, cracks, hot spots and other casting defects, thus resulting in sound castings.

1.2. Fracture toughness of cast iron

It is well-known that cast irons, unlike steels and non-ferrous alloys, are not homogeneous materials. They seem to behave more like composite materials than homogeneous metals or alloys ([1] p. 50). In fact, grey iron inherently contains innumerable notches and therefore has little or no sensitivity to the presence of additional notches resulting from design features ([1] pp. 21, 22). It follows, therefore, that it is extremely difficult to predict accurately the fracture behaviour of cast irons.

The usual microstructure of grey iron, fabricated by normal processes, is a matrix of pearlite with graphite flakes dispersed throughout the matrix. Foundry practice can be varied so that nucleation and growth of graphite flakes occur in a pattern that enhances the desired properties. The amount, size, and distribution of graphite are important parameters affecting the properties of the final product. Cooling that is too rapid tends to produce so-called chilled iron, in which the excess carbon is found in the form of massive carbides ([1] p.13). Furthermore, it has been documented that "when carbon equivalent values are relatively low or when cooling rates are relatively fast, the transformation to pearlite is favoured. In some instances, the microstructure will contain all these constituents: ferrite, pearlite, and graphite" ([1] p. 14). Because the present research involves rapid sub-zero chilling of cast iron, it is expected that pearlite will be present in all the test specimens. It would therefore be useful to ascertain if there is a relationship between the pearlite

0022–2461

content and the fracture toughness of the material, because this would provide a very convenient method for the prediction of the fracture properties of the material based on its microstructure.

1.3. Effect of chromium

When chromium is added to cast iron, a portion of it enters the iron carbide and forms complex Fe–Cr carbides. As chromium is added, the carbide present as a component of pearlite is first stabilized, and with further addition of chromium, primary or massive carbides are stabilized. One of the roles of chromium, therefore, is to act as a carbide stabilizer. Moreover, according to the American Foundry Society (AFS) Cast Metals Handbook [2], when small amounts of chromium are added to cast iron, ferritic structures are replaced by the stronger pearlitic types, the size of the graphite flakes is made more uniform, and the grain size is refined.

1.4. Relevance of this research

Cast iron is increasingly used today for highly stressed and critical components. The requirements concerning safety and reliability are always on the increase and therefore the resistance to fracture is ever more crucial. Because there are presently no published data on the fracture characteristics of sub-zero-chilled cast iron, the present research is intended to fill the void.

2. Experimental procedure

2.1. Fabrication of material

Cast-iron alloys of four different compositions were produced by casting at 1440 °C into the form of ingots, denoted Alloys A, B, C and D, with the compositions as shown in Table I. Apart from the usual alloying elements such as silicon, manganese, sulphur and phosphorus, copper was also added to enhance machinability as well as to act as a grain refiner. Chromium, being a carbide stabilizer, was added in compositions ranging from 0.00%–0.20%.

2.2. Casting procedure

To make the mould for casting, a teak wood pattern of size 225 mm by 150 mm by 25 mm was employed with standard pattern allowances. The moulds were prepared using silica sand with 5% bentonite as a binder and 5% moisture. The molten alloys were cast in the mould (as shown in Fig. 1) which was cooled from one end by a copper chill through which liquid nitrogen was passed. Molten metal was poured into the mould only after the liquid nitrogen had been allowed to circulate through the chill for a few minutes to stabilize the temperature. The temperature of the chill face of the mould was measured using a thermocouple and was found to be − 51 °C just before the molten metal was poured into the mould. Ingots were cast employing chills of different thicknesses (10, 15, 20 and 25 mm) in order to study the effect of the volumetric heat capacity (VHC) of the chill. The length and breadth of the chills were kept constant at 170 and 35 mm, respectively.

2.3. Specimen preparation

The specimens were prepared as per ASTM E 399-74. The specimens were taken from various locations in the casting, namely 25, 75, 150 and 225 mm from the chill end, the latter being situated at the riser end. The longitudinal axes of these specimens were parallel to the longitudinal axis of the copper chill during casting.

2.4. Fracture test procedure

All the fracture tests were done in conformance with ASTM E 399-74. The method of testing involves three-point bend testing of notched specimens which have been precracked by fatigue. The graph of load versus displacement across the notch at the specimen edge was recorded autographically. The load corresponding to 2% crack extension was established by a specific deviation from the linear portion of the record. From the load, the stress intensity factor, K_{IC} (which is a measure of the fracture toughness of the material), was calculated using equations which have been established on the basis of elastic–stress analysis. The validity of the determination of K_{IC} value by this method depends on the establishment of a sharp crack condition at the tip of the crack in a specimen of adequate size. All these conditions were fulfilled in these experiments.

2.5. Microstructural examination

Photomicrographs were taken of all the fracture test specimens to study their microstructures. Also, scanning electron micrographs were taken of all the fracture surfaces of the specimens to study the mode of fracture.

TABLE I Compositions of the cast iron alloys used

Alloy designation	Composition (wt %)							
	C	Si	Mn	S	P	Cu	Cr	Fe
A	3.42	1.8	0.41	0.04	0.08	1.5	0.00	Bal.
B	3.42	1.8	0.41	0.04	0.08	1.5	0.10	Bal.
C	3.42	1.8	0.41	0.04	0.08	1.5	0.15	Bal.
D	3.42	1.8	0.41	0.04	0.08	1.5	0.20	Bal.

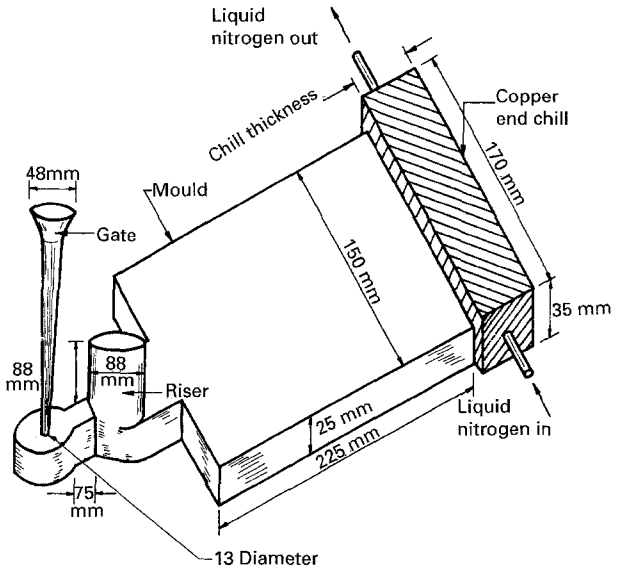

Figure 1 The mould for producing sub-zero-chilled cast iron.

TABLE II Fracture toughness test results for castings chilled by 10 mm thick chill

Specimen location (distance from chill, mm)	K_{IC} (MPa $m^{1/2}$)			
	Alloy A	Alloy B	Alloy C	Alloy D
25	32.6	32.8	33.2	35.8
75	29.7	30.2	31.2	32.8
150	28.1	29.2	27.2	27.8
225	22.8	22.8	22.8	22.7

3. Results and discussion

3.1. Fracture toughness

As expected, the scanning electron micrographs taken of the fracture surfaces of the specimens revealed a brittle mode of fracture in every case. The experimental results of the fracture toughness tests done on castings chilled using 10, 15, 20 and 25 mm thick chills are given in Tables II–V respectively.

Comparing the results in Tables II–V, it can be seen that changing the chill thickness seems to have only a very marginal effect on the fracture toughness of the casting. Nevertheless, there is a perceivable trend of increasing fracture toughness as the chill thickness is increased. This implies that increasing the rate of chilling tends to result in an increase in the fracture toughness of the material. Apparently, changing the chill thickness results in only a very slight change in the chilling rate.

Of more significant effect are the chromium content and the specimen location. It can be seen that if all other factors are kept constant, Alloy A invariably has the lowest fracture toughness, followed by Alloys B, C and D in that order. This means that increasing the chromium content results in an increase in the fracture toughness of the material. Moreover, the chromium content has greatest effect on specimens obtained 25 mm from the chill. As distance from the chill increases, the effect of chromium content greatly diminishes, implying that the effect of chromium is less significant if the rate of chilling is low.

TABLE III Fracture toughness test results for castings chilled by 15 mm thick chill

Specimen location (distance from chill, mm)	K_{IC} (MPa $m^{1/2}$)			
	Alloy A	Alloy B	Alloy C	Alloy D
25	32.8	32.9	33.2	37.8
75	30.4	30.8	32.8	35.2
150	23.5	28.6	27.2	27.2
225	22.8	22.7	22.8	22.7

TABLE IV Fracture toughness test results for castings chilled by 20 mm thick chill

Specimen location (distance from chill, mm)	K_{IC} (MPa $m^{1/2}$)			
	Alloy A	Alloy B	Alloy C	Alloy D
25	32.8	33.2	36.8	38.2
75	30.2	30.2	32.6	31.2
150	27.1	29.2	27.8	29.0
225	22.8	22.9	22.8	23.8

TABLE V Fracture toughness test results for castings chilled by 25 mm thick chill

Specimen location (distance from chill, mm)	K_{IC} (MPa $m^{1/2}$)			
	Alloy A	Alloy B	Alloy C	Alloy D
25	34.6	34.8	36.2	38.9
75	33.8	30.2	32.8	36.2
150	30.2	29.2	27.2	29.1
225	22.8	22.7	22.8	23.5

Moreover, the further away from the chill the specimen is taken, the lower is the fracture toughness. This could be because the further away from the chill the specimen is, the lower is the rate of chilling. This agrees with the deduction made earlier that increasing the rate of chilling tends to result in an increase in the fracture toughness of the material.

3.2. Effect of chromium content on microstructure

Typical photomicrographs of specimens taken at a distance of 25 mm from the chill end and produced using a 25 mm thick chill are shown in Figs 2–5. They were all etched with nital. Fig. 2 is a photomicrograph of Alloy A in which a small amount of cementite is seen in a matrix of pearlite. Fig. 3 is a photomicrograph of Alloy B in which 15%–20% cementite is seen in a matrix of pearlite. There is also some ledeburite visible. Alloy C, in which 20%–25% cementite is seen in a matrix of fine pearlite, is shown in Fig. 4, while Fig. 5 is a photomicrograph of Alloy D in which about 40% of cementite is seen in a matrix of lamellar pearlite. There is also about 10% ferrite visible. Apparently, therefore, the addition of chromium causes an increase in the cementite content, which concurs with the theory that chromium acts as a carbide stabilizer.

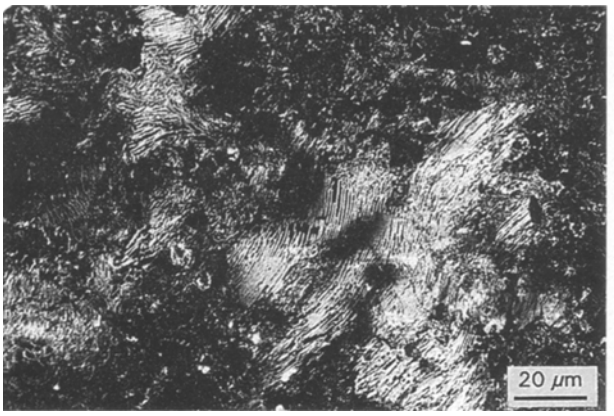

Figure 2 Photomicrograph of Alloy A specimen taken 25 mm from chill end and cast using a 25 mm chill.

Figure 5 Photomicrograph of Alloy D specimen taken 25 mm from chill end and cast using a 25 mm chill.

Figure 3 Photomicrograph of Alloy B specimen taken 25 mm from chill end and cast using a 25 mm chill.

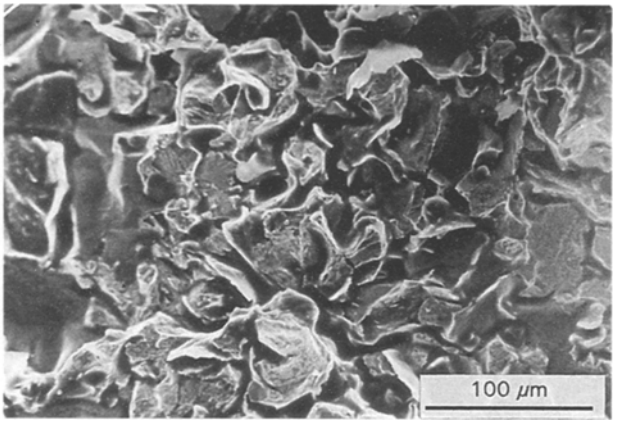

Figure 6 Fractograph of Alloy D specimen taken 30 mm from chill end and cast using a 25 mm chill.

Figure 4 Photomicrograph of Alloy C specimen taken 25 mm from chill end and cast using a 25 mm chill.

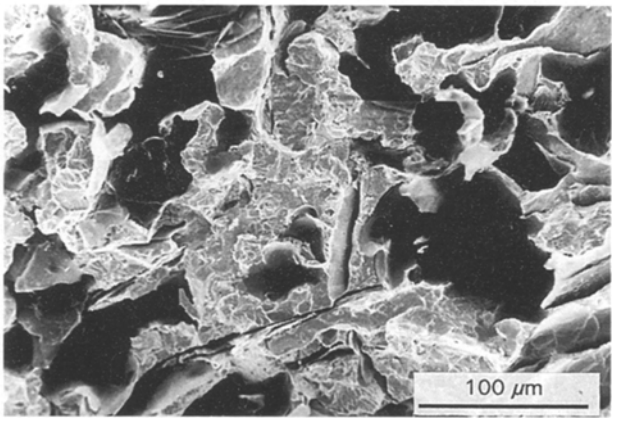

Figure 7 Fractograph of Alloy D specimen taken 70 mm from chill end and cast using a 25 mm chill.

3.3. Effect of specimen location on microstructure

Typical fractographs of specimens of Alloy D (which contains the highest chromium content) taken at various distances from the chill end and produced using a 25 mm thick chill (which gives the highest chilling rate) are shown in Figs 6–9. The specimen in Fig. 6 was taken 30 mm from the chill end. Stable crack growth and rupture of graphite flakes can be seen. The graphite present was of the rosette type (Type B). The fracture toughness was 33.88 MPa $m^{1/2}$ and the number of cycles to failure was 158 060. The pearlite content was 28%. The specimen in Fig. 7 was taken 70 mm from the chill end. Stable crack growth, void formation and ruptures of graphite flakes can be seen. The graphite present was of random orientation (Type A). The fracture toughness was 31.29 MPa $m^{1/2}$ and the number of cycles to failure was 163 893. The pearlite content was 35%. The specimen in Fig. 8 was taken 105 mm from the chill end. As before, stable crack growth, void formation and ruptures of graphite flakes can be seen. The graphite present was of random orientation (Type A). The fracture toughness was

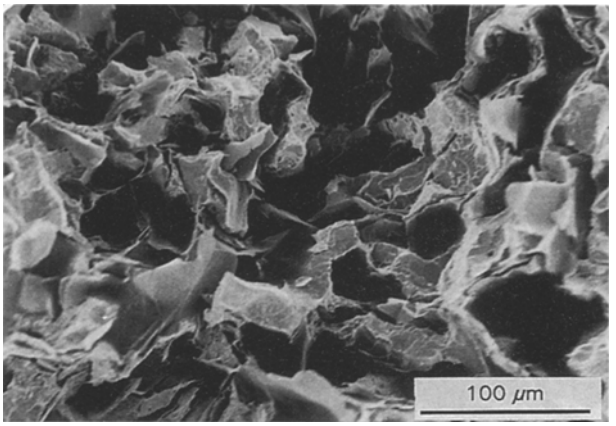

Figure 8 Fractograph of Alloy D specimen taken 105 mm from chill end and cast using a 25 mm chill.

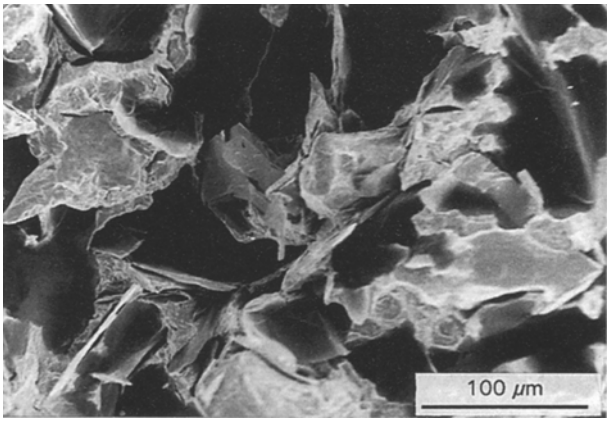

Figure 9 Fractograph of Alloy D specimen taken 210 mm from chill end and cast using a 25 mm chill.

29.10 MPa $m^{1/2}$ and the number of cycles to failure was 161 780. The pearlite content was 42%. Fig. 9 shows the specimen taken 210 mm from the chill end. Here, a cleavage mode of fracture of graphite flakes can be seen. The graphite present was of random orientation (Type A). The fracture toughness was 23.60 MPa $m^{1/2}$ and the number of cycles to failure was 118 256. The pearlite content was 68%.

These results clearly show that fracture toughness decreases with distance from the chill end. This is because the chill rate is highest at the chill end and decreases gradually as distance from the chill end is increased. The pearlite content is also seen to be affected significantly by the specimen location because the pearlite content increases with distance from the chill end. Speidel *et al.* [3] showed that ferritic cast irons exhibit significantly higher toughness values than the pearlitic cast irons. This was confirmed in our investigation, because at the chill end (corresponding to higher fracture toughness), some ferrite and some pearlite was observed. However, as the distance from the chill end is increased (corresponding to gradually decreasing fracture toughness), the ferrite content decreases to zero and the pearlite content increases to 100% near the riser end.

Tables VI–IX show comprehensively the percentages of ferrite (F), pearlite (P) and cementite (C) seen in the microstructures of all the specimens. From these tables it can be seen that as the distance from the chill end increases, the percentage pearlite increases at the expense of ferrite and cementite. In fact, at distances of 150 and 225 mm away from the chill end, no ferrite and cementite was detected. The drop in cementite content is much more remarkable than that in ferrite (because the ferrite content is always very small anyway, even at the chill end). This is because as the distance from the chill end increases, the chill rate decreases and there is more time for the graphite to precipitate out from the cementite, resulting in a marked decrease in cementite.

As chill thickness is increased from 10 mm to 25 mm, the ferrite content increases slightly but the cementite content increases significantly. Again, this observation can be explained by the fact that as the

TABLE VI Microstructural results for castings chilled by 10 mm thick chill., P, pearlite; C, cementite, F, ferrite

Specimen location (distance from chill, mm)	Composition (wt %)											
	Alloy A			Alloy B			Alloy C			Alloy D		
	P	C	F	P	C	F	P	C	F	P	C	F
25	41	3	2	39	5	2	36	10	5	32	20	8
75	52	0	0	48	0	0	44	0	0	39	0	0
150	64	0	0	62	0	0	59	0	0	58	0	0
225	71	0	0	71	0	0	71	0	0	70	0	0

TABLE VII Microstructural results for castings chilled by 15 mm thick chill

Specimen location (distance from chill, mm)	Composition (wt %)											
	Alloy A			Alloy B			Alloy C			Alloy D		
	P	C	F	P	C	F	P	C	F	P	C	F
25	39	8	2	38	10	3	36	15	6	29	25	8
75	49	2	0	47	2	2	42	5	4	38	5	2
150	68	0	0	63	0	0	59	0	0	59	0	0
225	71	0	0	70	0	0	70	0	0	71	0	0

TABLE VIII Microstructural results for castings chilled by 20 mm thick chill

Specimen location (distance from chill, mm)	Composition (wt %)											
	Alloy A			Alloy B			Alloy C			Alloy D		
	P	C	F	P	C	F	P	C	F	P	C	F
25	39	10	2	36	14	2	32	25	8	27	40	8
75	48	2	0	49	2	0	41	5	3	38	8	3
150	67	0	0	61	0	0	58	0	0	58	0	0
225	70	0	0	71	0	0	69	0	0	67	0	0

TABLE IX Microstructural results for castings chilled by 25 mm thick chill

Specimen location (distance from chill, mm)	Composition (wt %)											
	Alloy A			Alloy B			Alloy C			Alloy D		
	P	C	F	P	C	F	P	C	F	P	C	F
25	38	40	22	34	48	18	31	52	17	28	57	15
75	49	0	10	48	0	8	42	5	2	35	8	3
150	66	0	0	62	0	0	59	0	0	57	0	0
225	71	0	0	70	0	0	69	0	0	67	0	0

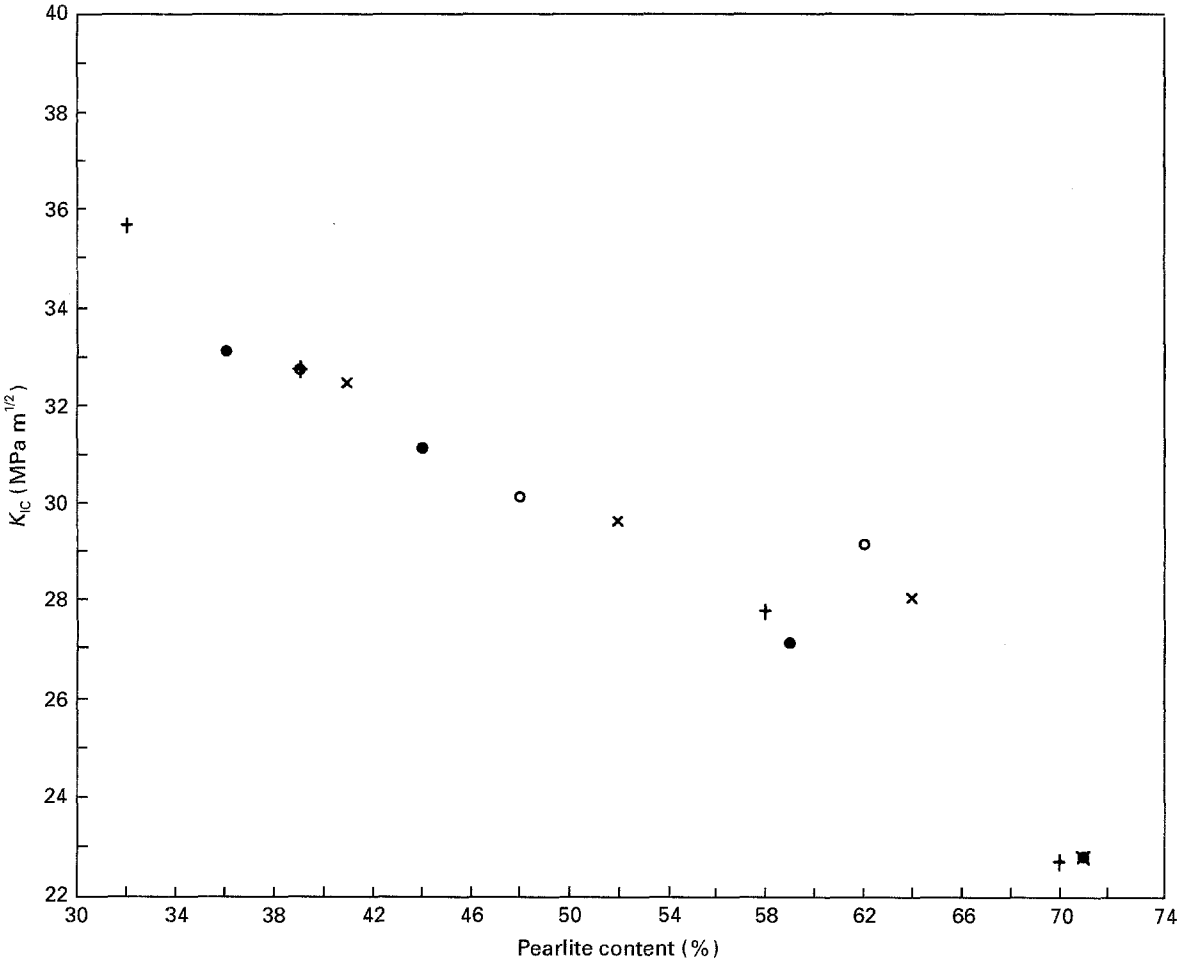

Figure 10 Graph of fracture toughness versus pearlitic composition for 10 mm thick chill. (×) Alloy A, (○) Alloy B, (●) Alloy C, (+) Alloy D.

chill thickness is increased, there is less time for the graphite to precipitate out from the cementite and hence more carbon remains locked within the cementite, resulting in the marked increase in cementite content.

Another observation is that as the chromium content is increased, so does the cementite content at the expense of pearlite. This was already highlighted earlier in the discussion of Figs 2–5, concurring with

the theory that chromium acts as a carbide stabilizer. There is, however, no consistent trend in the ferrite content as chromium content is increased.

3.4. Correlation between ferrite, pearlite and cementite contents and fracture toughness

It is noteworthy that the ferrite and cementite contents always increase together, at the expense of pearlite. Because the ferrite and cementite contents are too small to be measured in more than half the total number of specimens tested, it was much more convenient to plot a relationship between pearlite content and fracture toughness, as there was a significant amount of pearlite in every specimen. Moreover, because pearlite always increases at the expense of both ferrite and cementite, such a plot would also indicate the relative amounts of these two latter phases therein.

3.4.1. Relationship between pearlite content and fracture toughness

From the above results, therefore, it can be deduced that there is a very straightforward reciprocal relationship between pearlite content and fracture toughness. In other words, fracture toughness decreases with increase in the proportion of pearlite present in the material and vice versa. This is in agreement with the theories put forward by other researchers [3].

If the fracture toughness results obtained using a 10 mm thick chill shown in Table II are plotted against the corresponding pearlite compositions shown in Table VI, the 16 points are seen to follow a roughly linear relationship (Fig. 10). If the same procedure is done for the results obtained using a 25 mm chill (Tables V and IX), an approximate linear relationship is perceived as well (Fig. 11). The chromium content of the material does not seem to be of any noticeable consequence because all the points (whether for Alloy A, B, C or D) seem to follow this relationship in both Figs 10 and 11.

Furthermore, if all the 64 values of fracture toughness shown in Tables II–V and the 64 values of pearlite content shown in Tables VI–IX are plotted on to a single graph of fracture toughness versus pearlite content, an approximate linear relationship between these two properties can be seen (Fig. 12). It is noteworthy too that the 64 points represent sub-zero-chilled cast iron of varying chromium composition and different rates of chilling. Apparently, therefore, no matter what the chromium content or the rate of chilling, there is a marked correlation between the fracture toughness and the pearlite content for sub-zero-chilled cast iron. This relationship will be useful for predicting the fracture toughness of the material when the pearlite content is known from microscopic examination.

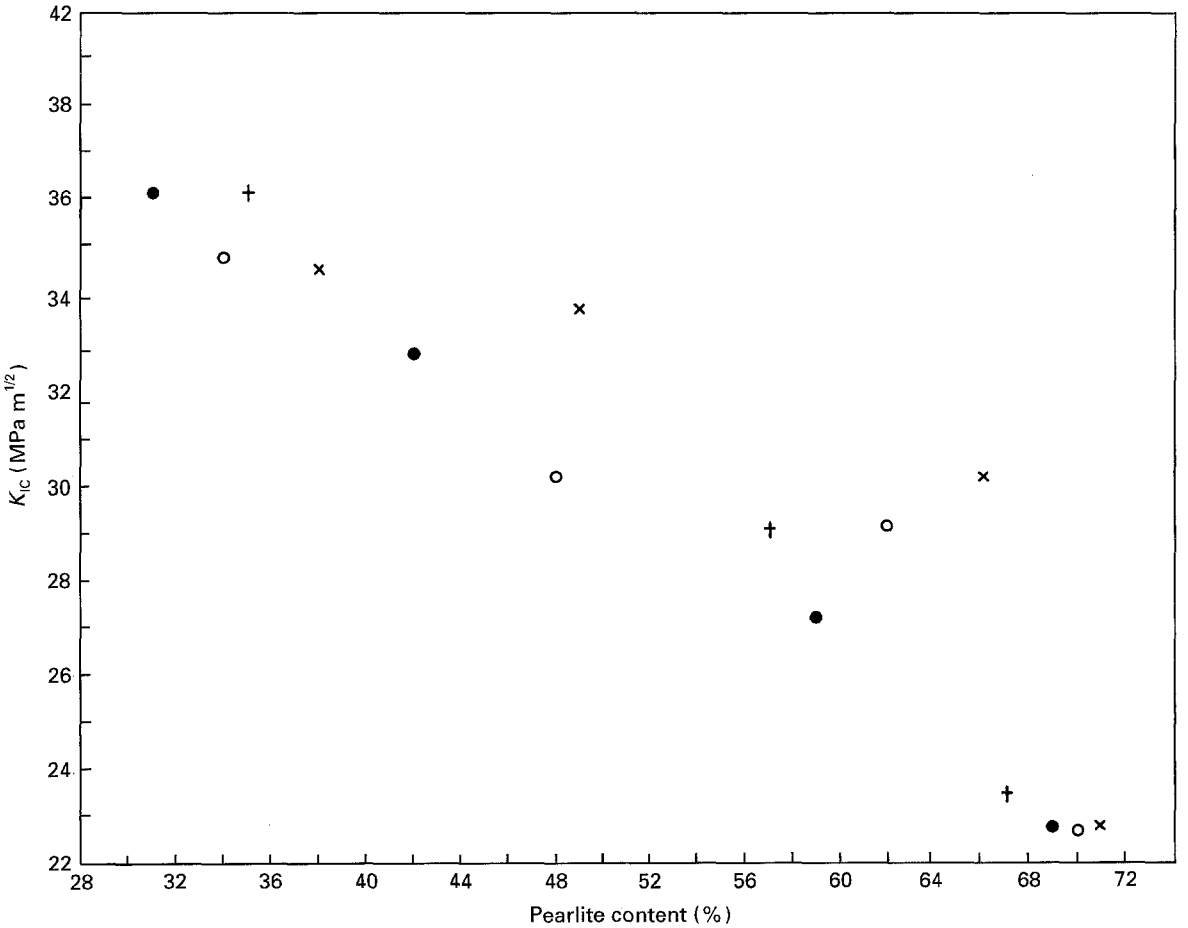

Figure 11 Graph of fracture toughness versus pearlitic composition for 25 mm thick chill. For key, see Fig. 10.

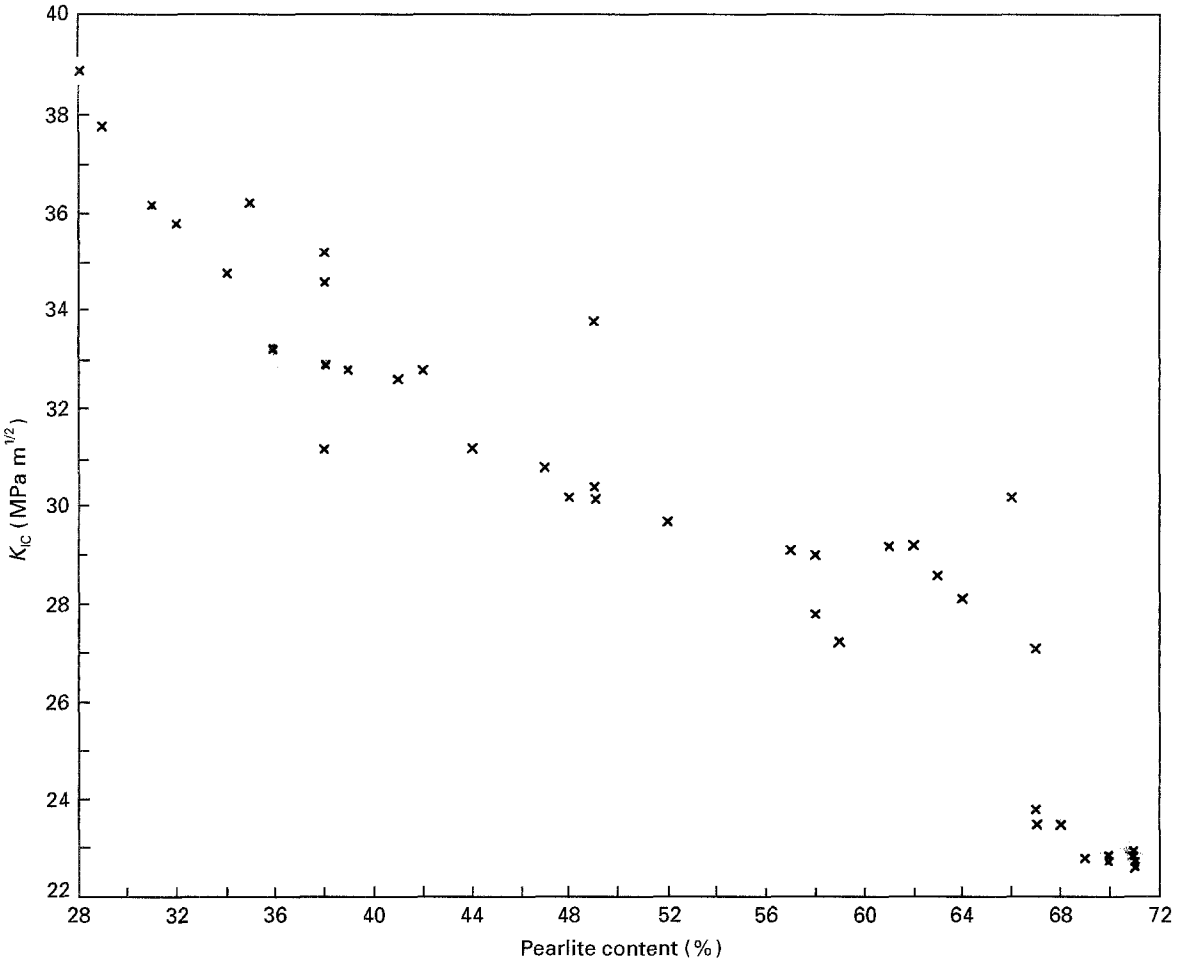

Figure 12 Complete graph of fracture toughness versus pearlitic composition.

4. Conclusion

The fracture toughness of sub-zero-chilled cast iron is highly dependent on the chilling rate as well as the chromium content of the material. Increase in the rate of chilling and increase in the chromium content of the material both result in an increase in the fracture toughness due to a decrease in the pearlite content. However, the effect of chromium content is less significant if the rate of chilling is low. The fracture toughness of sub-zero-chilled cast iron is significantly affected by the pearlite content in the material. There is an approximately linear relationship between these two properties, in which fracture toughness decreases as the pearlite content increases and vice versa. This relationship will be useful for predicting the fracture toughness of the material when the pearlite content is known from microscopic examination.

References

1. "Metals Handbook", Vol. 1, "Properties and selection: irons, steels and high-performance alloys" (ASM International, 10th Edn 1990).
2. "AFS Cast Metals Handbook", 4th Edn (AFS, Des Plaines, IL 1975) p. 87.
3. M. O. SPEIDEL, S. WOLFENSBERGER and P. J. UGGOWITZER, *Ind. Found. J.* **35** (1984) 15.

Received 3 May 1994
and accepted 11 April 1995